Cardiovascular Dynamics during Head-up Tilt assessed Via a Pulsatile and Non-pulsatile Model

N. Williams, H. T. Tran and M. S. Olufsen
Department of Mathematics, NC State University, Raleigh, NC, U.S.A.

Keywords: Cardiovascular Dynamics Modeling, Head-up Tilt, Pulsatile vs. Non-pulsatile Modeling, Parameter Estimation.

Abstract: This study compares a pulsatile and a non-pulsatile model for prediction of head-up tilt dynamics for healthy young adults. Many people suffering from dizziness or light-headedness are often exposed to the head-up tilt test to explore potential deficits within the autonomic control system, which is supposed to maintain the cardiovascular system at homeostasis. However, this system is complex and difficult to study in vivo. This study shows how mathematical modeling can be used to extract features of the system that cannot be measured experimentally. More specifically, we show that it is possible to develop a mathematical model that can predict changes in cardiac contractility and vascular resistance, quantities that cannot be measured directly, but which can be useful to assess the state of the system. The cardiovascular system is pulsatile, yet predicting control in response to head-up tilt for the complete system is computationally challenging, and limits the applicability of the model. In this study we show how to develop a simpler non- pulsatile model that can be interchanged with the pulsatile model, which is significantly easier to compute, yet it still is able to predict internal variables. The models are validated using head-up tilt data from healthy young adults.

1 INTRODUCTION

Emergency rooms and syncope clinics see a large number of people who have experienced lightheadedness or dizziness. These syndromes may be associated with orthostatic intolerance: the inability to maintain blood pressure and flow in response to active standing or head-up tilt. Orthostatic intolerance (Lanier et al., 2011) is triggered by a number of factors, the most important being dysautonomia, a disorder associated with the autonomic nervous system.

In this study we use mathematical modeling to predict blood pressure and heart rate dynamics observed during HUT. The HUT protocol starts with a subject resting in supine position on a tilt-table, after steady oscillating values for heart rate and blood pressure have been recorded, the subject is tilted head up to a 60-70 degree angle. The test typically lasts between 10-20 minutes after initiation of the tilt. At this point most subjects feel light-headed and are tilted back to supine position. Upon tilting blood is pooled in the lower body causing a drop in blood pressure in the upper body, while blood pressure in the lower body is increased. In response (for healthy subjects), the autonomic system causes an increase in heart rate, cardiac contractility, and peripheral resistance redistributing blood volume and thereby reestablishing homeostasis. For patients suffering from dysautonomia, these responses may be partly or completely inhibited.

More specifically, this paper compares a pulsatile and a non-pulsatile mathematical model that can predict cardiovascular dynamics during HUT. Although a pulsatile model for the cardiovascular system is beneficial, it enables analysis of dynamics within beats and can be used to understand how modulation of the system affects pulsatility (Williams et al., 2013), which is useful in the study of the response immediately following HUT (within minutes of the tilt). However, for numerous problems it is adequate to analyze the system with the simpler non-pulsatile model. For example, if the objective is to study dynamics associated with the entire procedure (10-20 min). In this study we develop a non-pulsatile model for the cardiovascular system that can predict HUT dynamics, and show that parameters estimated with the non-pulsatile model can be used within the pulsatile model or possibly be combined with more complex models including spatial information.

Williams N., T. Tran H. and S. Olufsen M..
Cardiovascular Dynamics during Head-up Tilt assessed Via a Pulsatile and Non-pulsatile Model.
DOI: 10.5220/0004624006730680
In *Proceedings of the 3rd International Conference on Simulation and Modeling Methodologies, Technologies and Applications* (BIOMED-2013), pages 673-680
ISBN: 978-989-8565-69-3

Besides being able to interchange the non-pulsatile and pulsatile models, in itself non-pulsatile models have multiple advantages. First, since they are less complex, coupling a non-pulsatile model with more advanced models studying larger systems such as the respiratory or renal systems becomes feasible. Moreover, with a simple model it becomes possible to study system dynamics over much longer time-scales (hours-days). The respiratory cycle is approximately a fourth of the cardiovascular cycle, and control associated with respiratory dynamics take min-hours (Hall, 2011). The renal system is one of the most complex physiological feedback systems, it interacts with the cardiovascular system, and feedback associated with this system is hours-days (Hall, 2011). Even if the objective is to study the impact of fainting, often studied using HUT tests, it may be necessary to use a simpler model. Typically, after HUT it takes 10-20 minutes before the subject tilted experiences light headedness (Lanier et al., 2011). Finally, it should be emphasized that computations with the non-pulsatile are significantly faster, in particular, since it is no longer necessary to account for the discrete events associated with opening and closing of the heart valves. In the following we will present both a pulsatile and a non-pulsatile model and show that they can be used interchangably in the study of HUT dynamics.

2 METHODS

This section describes both the pulsatile and non-pulsatile models, as well as the model changes imposed to predict gravitational pooling and autonomic regulation necessary to predict HUT dynamics. We first describe the two models, we discuss HUT, and methods needed for comparing model predictions.

2.1 Data

As a point of departure we use the model and modeling results presented in (Williams et al., 2013), which develops and validates a pulsatile model predicting HUT dynamics for five healthy young subjects. Since our objective is to develop a non-pulsatile model using the same framework as the pulsatile model, we modify the heart compartment, while the remaining model compartments stay the same. To compare the two models, we predict the moving average of the pressures, cardiac output, and total blood volume from the pulsatile model and compare results with the non-pulsatile model. Comparisons are done using sensitivity analysis, subset selection, and optimization. More specifically, we estimate a set of model parameters minimizing the least squares error between states computed by the two models. Only parameters that represented differences between the two models (i.e., the heart component) are allowed to vary.

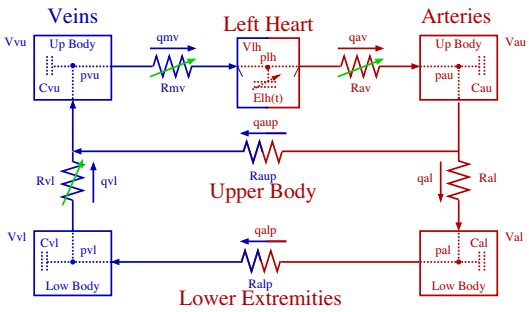

Figure 1: Compartment model predicting HUT dynamics. For each compartment an associated blood pressure p (mmHg), volume V (ml), and compliance C (ml/mmHg) are defined. The compartments represent the upper body arteries (subscript *au*), lower body arteries (subscript *al*), upper body veins (subscript *vu*), lower body veins (subscript *vl*), and the left heart (subscript *lh*). Resistances R (mmHg s/ml) are placed between all compartments: R_{al} denotes the resistance between arteries in the upper and lower body, R_{aup} and R_{alp} denote resistance between arteries and veins in the upper and lower body, respectively. For the pulsatile model, the two heart valves, the mitral valve and the aortic valve, are modeled as pressure dependent resistors R_{mv} and R_{av}. Finally, the resistance between the lower and upper body veins R_{vl} is also modeled as pressure dependent to prevent retrograde flow into the lower-body during the HUT.

2.2 Lumped Cardiovascular Models

This section describes the pulsatile and non-pulsatile cardiovascular models depicted in Figure 1. These models are developed to estimate blood flow, volume, and pressure in the systemic circulation during HUT with and without a pulsating heart. Similar to the pulsatile model (Williams et al., 2013), the non-pulsatile model development is split into parts including development of a lumped cardiovascular model estimating dynamics while the subject is resting in supine position; developing model components allowing prediction of dynamic changes to HUT; and development of methods for estimating the impact of cardiovascular regulation on the model parameters.

Both models follow the same basic layout shown in Figure 1, including four compartments representing arteries and veins in the upper and lower body and a compartment representing the heart. The latter, is the only compartment that differ between the two models. Therefore, the general equations outlined below are valid for both models.

For each compartment, a pressure-volume relation

can be defined as

$$V_i - V_{un} = C_i(p_i - p_{ext}), \tag{1}$$

where V_i (ml) is the compartment volume, V_{un} (ml) is the unstressed volume, C_i (ml/mmHg) is the compartment compliance, p_i (mmHg) is the compartment instantaneous blood pressure, and p_{ext} (mmHg) (assumed constant) is the pressure in the surrounding tissue. Moreover, for each compartment, the change in volume is given by

$$\frac{dV_i}{dt} = q_{in} - q_{out}, \tag{2}$$

where q (ml/s) denotes the volumetric flow. Using a linear relationship analogous to Ohm's law the volumetric flow q (ml/s) between compartments can be computed as

$$q = \frac{p_{in} - p_{out}}{R}, \tag{3}$$

where p_{in} and p_{out} are the pressure on either side of the resistor R (mmHg s/ml). Differentiating (1), using (2), and inserting (3) allows us to obtain a system of differential equations in blood pressure of the form

$$\frac{dp_i}{dt} = \frac{1}{C_i}\frac{dV_i}{dt} = \frac{1}{C_i}\left(\frac{p_{i-1} - p_i}{R_{i-1}} - \frac{p_i - p_{i+1}}{R_i}\right),$$

where i refer to the compartment for which the pressure p_i is computed, while $i-1$ and $i+1$ refer to the two neighboring compartments. For resistances that appear between compartments, R_{i-1} refer to the resistance between compartments $i-1$ and i, and R_i refer to the resistance between compartments i and $i+1$. The latter equation is valid since we assume that C_i (ml/mmHg) is constant. This formulation is utilized for the four arterial and venous compartments.

For the pulsatile model, (2) describes the change in volume of the left heart. Using a relation similar to (1) we get

$$p_{lh} = E_{lh}(V_{lh} - V_{un}), \tag{4}$$

where E_{lh} (mmHg/ml) is the left heart elastance (the reciprocal of its compliance) and V_{lh} is the left heart volume. Pumping is achieved by introducing a variable elastance function (Ellwein, 2008) of the form

$$E_{lh}(\tilde{t}) = \tag{5}$$
$$\begin{cases} \frac{E_M - E_m}{2}(1 - \cos(\frac{\pi\tilde{t}}{T_M}) + E_m), & \tilde{t} \le T_M \\ \frac{E_M - E_m}{2}(\cos(\frac{\pi(\tilde{t} - T_M)}{T_R}) + 1) + E_m, & \tilde{t} \le T_M + T_R \\ E_m, & \tilde{t} \le T \end{cases}$$

where $\tilde{t}$ is the time within a cardiac cycle $T = 1/H$. E_m and E_M denote the minimum and maximum elastance, respectively. For each cardiac cycle elastance is increased for $0 < \tilde{t} < T_M$ and decreased for $T_M < \tilde{t} < T_M + T_R$, while during diastole $T_M + T_R < \tilde{t} < T$ elastance is kept constant at its minimum value. Values for T and T_M are obtained from data, while T_R is a model parameter.

Finally, heart valves are modeled using pressure dependent resistors for which a large resistance R_{cl} represents a closed valve, while a small resistance R_{op} represents an open valve. These are modeled as smooth sigmoidal functions of the form

$$R_v = R_{cl} - \frac{R_{cl} - R_{op}}{1 + e^{-\beta(p_{in} - p_{out})}}, \tag{6}$$

where p_{in} and p_{out} denote the pressures in compartments on either side of the valve. For $p_{in} > p_{out}$, $R_v \to R_{op}$ (the valve is open), and when $p_{out} > p_{in}$, $R_v \to R_{cl}$ (the valve closes).

The non-pulsatile heart model is adapted work by Batzel et al. (Batzel et al., 2007), which followed ideas originally proposed by Grodins (Grodins, 1959). This method does not explicitly model the pumping of the heart, but predicts cardiac output Q as a function of venous pressure p_v. The original model was used within a complete circulation. It predicted cardiac output as a function of pulmonary venous pressure, the current model only encompasses the systemic circulation, consequently this study predicts cardiac output as a function of systemic venous pressure p_{vu}.

The basic assumption concerning cardiac output, i.e., the outflow of blood from the heart, for non-pulsatile flow states that: Given the heart rate H (in strokes per minute) the flow of the left ventricle Q generated by a ventricle is given by

$$Q = HV_{str}, \tag{7}$$

where V_{str} is the stroke volume, i.e., the volume of blood ejected during one stroke. As a result time varying quantities in the non-pusatile model are to be interpreted as averages over the length of a pulse. The stroke volume is given by

$$V_{str} = V_{ED} - V_{ES}, \tag{8}$$

where V_{ED} is the end-diastolic volume and V_{ES} is the end-systolic volume of the heart.

Another assumption involves expressing stroke volume V_{str} as a function of the arterial and venous pressures acting on the ventricle. Concerning the ejection phase of the heart cycle we have the so called Frank-Starling mechanism (Burton, 1972), which states that the stroke volume of the heart increases in response to an increase in the volume of blood filling the heart (the end diastolic volume) when all other factors remain constant. Consequently, increased filling of the ventricle during diastole, causes an increased contraction force during the following

systole.

$$V_{str} = \frac{S}{p_a}(V_{ED} - Vun), \tag{9}$$

where p_a is the arterial pressure against which the ventricle has to eject (the afterload) and S denotes the contractility of the left ventricle.

Using the previous two assumptions we express the ventricular output Q (the cardiac output) as a function of blood pressure. To model the filling process of the heart, when the mitral valve is open, we assume that the inflow in to the ventricle depend on the difference between the filling pressure and the left ventricle pressure, using an expression analogous to (3), we get

$$\dot{V}_{lh}(t) = \frac{1}{R_{lh}}(p_v - p_{lh}), \tag{10}$$

where V_{lh} is the ventricular volume at time t after the filling process has started, p_{lh} is the ventricular pressure, p_v is the venous filling pressure assumed to be constant, and R_{lh} is the total ventricular resistance to the inflow of blood.

For the relaxed ventricle, a similar volume-pressure relation can be derived (e.g., as in (1)),

$$V(t) = C_{lh}p_{lh}(t) + V_{un}, \tag{11}$$

where V_{un} denotes the unstressed volume of the relaxed ventricle and C_{lh} denotes the heart compliance. The initial value for (10) is given by $V(0) = V_{ES}$. Using (11) in (10), integrating, and letting $t = t_d$, the time of end-diastole, we obtain

$$V_{ED} = kV_{ES} + a(C_{lh}p_v + V_{un}), \tag{12}$$

where $k = \exp(-t_d/C_{lh}R_{lh})$ and $a = 1-k$.

Equations (8), (9), and (12) constitute a system of linear equations for V_{ED}, V_{ES}, and V_{str}. We obtain

$$V_{ED} = C_{lh}p_v + V_{un} - \frac{C_{lh}kp_vS}{ap_a + kS}, \tag{13}$$

$$V_{ES} = C_{lh}p_v + V_{un} - \frac{C_{lh}p_vS}{ap_a + kS}, \tag{14}$$

$$V_{str} = \frac{aC_{lh}p_vS}{ap_a + kS}. \tag{15}$$

Combining (7) and (15) gives the cardiac output out of the ventricle

$$Q = H\frac{aC_{lh}p_vS}{ap_a + kS}, \tag{16}$$

where H is heart rate, C_{lh} heart compliance, p_v venous pressure, $p_a$arterial pressure, and S contractility.

There are essentially two possibilities for a ventricle to change the cardiac output: to change the heart rate or the contractility. Heart rate and contractility are related through the Bowditch effect (Klabunde, 1972), which states that contractility is proportional to heart rate. The Bowditch effect can be accounted for by introducing the second order ordinary differential equation, of the form

$$\ddot{S} + \gamma\dot{S} + \alpha S = \beta H, \tag{17}$$

where γ, α, and β are positive constants and H is heart rate. For this study, we rewrite this second order ODE as two first order equations.

Using these relations the pulsatile five differential equations can be written as

$$\begin{aligned}
\frac{dp_{au}}{dt} &= (q_{av} - q_{al} - q_{aup})/C_{au} \\
\frac{dp_{al}}{dt} &= (q_{al} - q_{alp})/C_{al} \\
\frac{dp_{vl}}{dt} &= (q_{alp} - q_{vl})/C_{vl} \\
\frac{dp_{vu}}{dt} &= (q_{aup} + q_{vl} - q_{mv})/C_{vu} \\
\frac{dV_{lh}}{dt} &= q_{mv} - q_{av}
\end{aligned}$$

and the non-pulsatile equations as

$$\begin{aligned}
\frac{dp_{au}}{dt} &= (Q - q_{al} - q_{aup})/C_{au} \\
\frac{dp_{al}}{dt} &= (q_{al} - q_{alp})/C_{al} \\
\frac{dp_{vl}}{dt} &= (q_{alp} - q_{vl})/C_{vl} \\
\frac{dp_{vu}}{dt} &= (q_{aup} + q_{vl} - Q)/C_{vu}, \\
\frac{dS}{dt} &= \sigma \\
\frac{d\sigma}{dt} &= -\alpha S - \gamma\sigma + \beta H,
\end{aligned}$$

where

$$\begin{aligned}
q_{av} &= \frac{p_{lh} - p_{au}}{R_{av}} \\
q_{aup} &= \frac{p_{au} - p_{vu}}{R_{aup}} \\
q_{al} &= \frac{p_{au} - p_{al}}{R_{al}} \\
q_{alp} &= \frac{p_{al} - p_{vl}}{R_{alp}} \\
q_{vl} &= \frac{p_{vl} - p_{vu}}{R_{vl}} \\
q_{mv} &= \frac{p_{vu} - p_{lh}}{R_{mv}}.
\end{aligned}$$

In the last set of equations the left ventricular pressure (p_{lh}) is predicted using (4), the pressure dependent resistances used to model the valves (R_{av}, R_{mv}) are predicted from (6), and the total blood volume can be

computed from pressures using (1). These equations were solved in Matlab using the ODE15s differential equations solver. Abbreviations (subscripts) are given in Table 1.

2.2.1 Modeling HUT

As the subject is tilted (shown in Figure 2), blood is pooled in the lower extremities leading to an increase in pressure in the lower body, while pressure in the upper body decreases. To account for gravity, the pressure at the level of the carotid arteries are used as a reference pressure, so an extra term is added to the flow (q_{al}) and subtracted from the flow (q_{vl}) of the lower body compartments. The gravitational effects are calculated as described by Olufsen et al. (Olufsen et al., 2005; Williams et al., 2013), giving the following modified flow equations

$$q = \frac{\rho g h_{tilt} \sin(\theta(t)) + p_{in} - p_{out}}{R}, \quad (18)$$

$$\theta(t) = \frac{\pi}{180} \begin{cases} 0 & t < t_{st} \\ v_t(t - t_{st}) & t_{st} \le t \le t_{st} + t_{ed} \\ 60 & t > t_{st} + t_{ed} \end{cases}$$

where ρ (g/ml) is blood density, g (cm/s^2) is the constant of gravitational acceleration, h_{tilt} (cm) is the absolute height between the upper body and lower body compartments, $\theta(t)$ is the tilt angle (in radians), $v_t = 15$ degrees/s is the tilt speed, while t_{st} and t_{ed} denote the time at which HUT is started and ended, respectively. The combined term $\rho g h_{tilt} \sin(\theta(t))$ denotes the hydrostatic pressure between the upper and lower body compartments.

2.2.2 Modeling Effects of Cardiovascular Regulation

Upon HUT firing of the baroreceptor nerves are modulated by the aortic and carotid sinus baroreceptors sensing changes in the stretch of the arterial wall. Typically, HUT leads to a decrease in blood pressure mediating an increase in sympathetic outflow along

Table 1: Abbreviations (subscripts) used in the compartmental model.

Abbreviation	Name
av	aortic valve
au	upper body arteries
al	lower body arteries
aup	upper body "peripheral" vascular bed
alp	lower body "peripheral" vascular bed
vu	upper body veins
vl	lower body veins
lh	the left heart (ventricle and atrium)

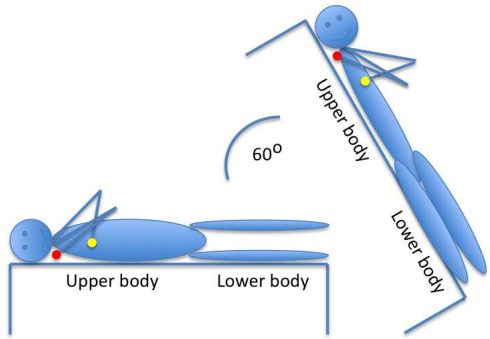

Figure 2: The HUT test: The subject depicted is tilted to an angle of 60 degrees at a constant speed of 15 degrees per second. Red and yellow circles indicate the locations for the blood pressure sensors. Each sensor is mounted on the index finger, one finger (red) is placed at the level of the carotid artery, while the other (yellow) is placed at the level of the heart. Upon HUT blood is pooled in the lower extremities.

with parasympathetic withdrawal. Sympathetic stimulation elicits changes in vascular resistance and cardiac contractility, while parasympathetic withdrawal primarily has an effect on heart rate and cardiac contractility. Heart rate is used as an input, consequently, parasympathetic heart rate regulation is implicitly accounted for in the model. For the pulsatile model, regulation of cardiac contractility is modeled by controlling the minimum elastance of the left heart (E_m) and vascular resistance is regulated in both the upper and lower body. However, as the compartments representing the upper and lower body arteries appear in parallel, both resistances are not identifiable. We controlled R_{aup} directly, while we let $R_{alp} = kR_{aup}$, where k is the ratio of the optimized supine values of R_{aup} and R_{alp}. For the non-pulsatile model, we do not have an explicit expression for E_m, instead contractility is included via the Bowditch effect (Klabunde, 1972), and modeled as a function of heart rate as described in (17). Hence, changes in contractility has been modeled indirectly, via the 2'nd order ODE, while parameters associated with autonomic control of vascular resistance should be modeled. To so, similar to (Williams et al., 2013) we predict R_{aup} as a piece-wise linear function given by

$$X(t) = \sum_{i=1}^{N} \gamma_i K(t), \quad (19)$$

$$K(t) = \begin{cases} \frac{t - t_{i-1}}{t_i - t_{i-1}}, & t_{i-1} \le t \le t_i \\ \frac{t_{i+1} - t}{t_{i+1} - t_i} & t_i \le t \le t_{i+1} \\ 0, & \text{otherwise} \end{cases}$$

where the unknown coefficients γ_i, $i = 1 \ldots N$ are the new parameters that will be estimated to predict the

control. N is the number of nodes along the time span analyzed. The spread of the N nodes should be specified in the model. For simulations reflecting dynamics observed in supine position we placed the nodes with a frequency of 6-10 seconds, but during HUT, where dynamics change, significantly more points are added. It should be noted that the more points are added to the time-span, the longer the simulations.

3 RESULTS

We first show results obtained for a subject in supine position followed by results obtained when the same subject is tilted upright to a 60 degree angle (see Figure 2). Results during supine position are included to tune model parameters to the subject studied, while during HUT we allow parameters regulated by the autonomic control system to vary in time. For each event we estimate parameters minimizing the least squares error between the model output and data. To develop two models (pulsatile and non-pulsatile) that can be interchanged, we compute moving averages for the quantities $X = \{p^m_{au}, p^m_{vu}, p^m_{al}, p^m_{vl}, CO^m, V^m_{tot}\}$ using pulsatile model outputs predicted in Williams et al. (Williams et al., 2013), and use these as data for the non-pulsatile model.

3.1 Optimization During Supine Position

First we predict dynamics during supine position, as stated above. These simulations are included to tune the model to the subject studied. For these simulations we estimate parameters in the non-pulsatile heart model (R_{lh}, C_{lh}, α, β, γ, c) minimizing the least squares error

$$J = \frac{1}{N}\sum_{i=1}^{N}\left(\frac{X_i^d - X_i^m}{X_i^d}\right)^2,$$

where X denotes the states listed above, superscript d refers to the data (obtained from the pulsatile model (Williams et al., 2013)), and superscript m refers to results obtained with the non-pulsatile model.

It should be noted that parameters "not" associated with the heart compartment are kept constant, since they represent components common for the two models. Results comparing the pulsatile and non-pulsatile model during steady state are shown in Figure 3. This figure shows all pressures and cardiac output. Each graph shows pulsatile model results (from Williams et al. (Williams et al., 2013)), moving

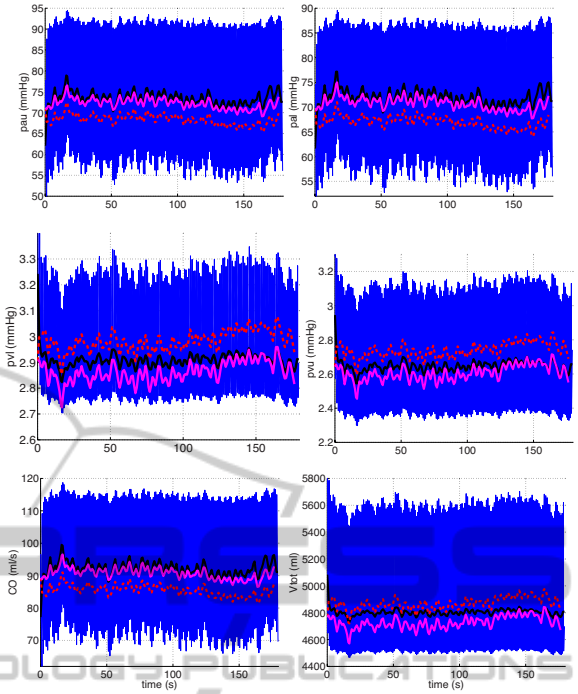

Figure 3: Predictions during supine position. All graphs include the pulsatile model output (blue), the mean of the pulsatile model output (black), the non-optimized (red, dashed) and optimized (magenta) non-pulsatile model output for the upper and lower body arterial pressure p_{au} and p_{al}, upper and lower body venous pressure p_{vu} and p_{vl}, cardiac output CO, and total volume V_{tot}.

averages predicted from the pulsatile model (black line), computations with the non-pulsatile model using nominal parameters (red dashed line), and computations with optimized parameters for the non-pulsatile model (magenta line). Note that for all states the two models agree well.

Initial parameters used for the arterial and venous portions of the model (results not shown) were estimated as described in previous studies Williams et al. (Williams et al., 2013). In short, we used sensitivity analysis and subset selection to obtain a set of parameters that can be estimated given the model and available data, and used nonlinear optimization to estimate their value. For this study, we only estimated parameters associated with the heart component within the non-pulsatile heart, assuming the tuned arterial and venous parameters found within the pulsatile model can be used within both formulations.

3.2 HUT Optimization

Once baseline parameters were obtained, we imposed HUT, by modifying flows between the upper and lower body as described in (18). For these simula-

tions, we only estimate the control parameters $\theta = \gamma_{Raup,i}$ used for computing R_{aup} as stated in (19), i.e., we let the parameter R_{sup} vary in time. In the pulsatile model we also let contractility be time-varying, via estimation of $\gamma_{Em,i}$, yet the non-pulsatile model directly accounts for this part of the control via the Bowditch effect (17), predicting cardiac contractility S as a function of heart rate H. For this portion of the model, we only included p_{au} in the cost function, giving

$$J = \frac{1}{N}\sum_{i=1}^{N}\left(\frac{p^d_{au,i} - p^m_{au,i}}{p^d_{au,i}}\right)^2,$$

where superscript d refers to the data and superscript m for the model.

Figure 4 shows the pulsatile model output (blue), the moving average data computed from the pulsatile model (black), and results using nominal parameter values (red dashed) during HUT. The subject is tilted after 80 sec and remains upright for the duration of the simulation. The top left graph in Figure 4 depicts dynamics without activating the control, i.e., for this simulation R_{aup} is kept at its baseline value. Note that after about 100 sec, this part of the model deviates slightly from results obtained with the pulsatile model. This is likely due to the fact that the non-pulsatile model results already incorporate control of contractility (S), while the "data" obtained from the pulsatile model were obtained using constant contractility values E_m. The following graphs show all model predicted pressures obtained with the non-pulsatile model using optimal parameter values. Note that predictions for p_{au} are significantly closer than for the other states, this is likely because for these simulations, we only include p_{au} in the cost function. In other words, no effort was made to account for variation in the remaining states. Finally, Figure 5 shows corresponding volumes and cardiac output, both are shown with nominal and optimized parameter values. This figure also shows time-varying prediction of peripheral vascular resistance R_{sup}.

The significance of the relation between the pulsatile and non-pulsatile models are corroborated further by examining dynamics of quantities for which data are not available, i.e., for p_{vu}, p_{al}, and p_{vl} depicted in Figure 4. Finally, our model provides good predictions of blood volume and cardiac output, depicted for a representative subject in Figure 5.

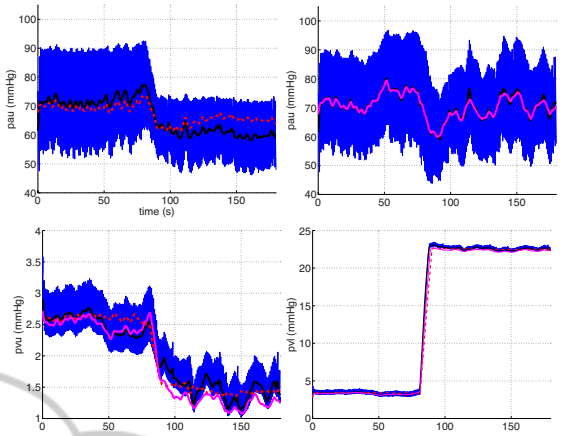

Figure 4: Predictions during HUT. Pulsatile (blue), moving average from pulsatile model (magenta), non-pulsatile model with nominal (red dashed) and optimized (magenta) parameter values. The top graph shows p_{au} predicted using nominal parameter values. The following four panels compares arterial and venous pressures in the upper and lower body.

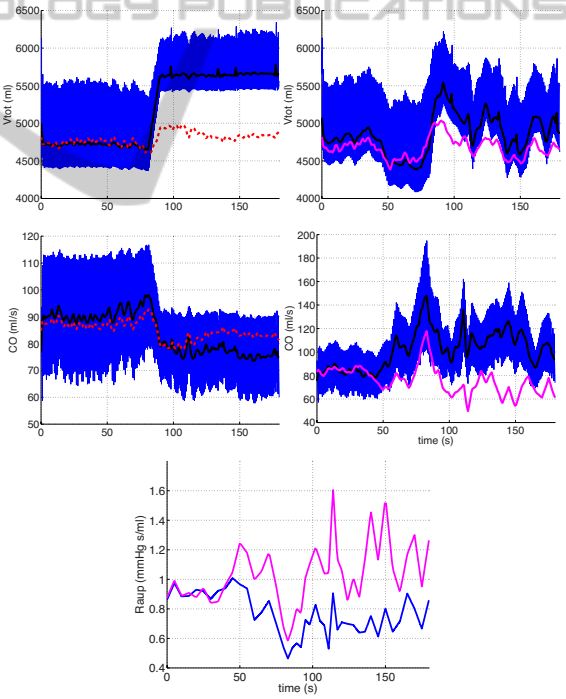

Figure 5: Volume and CO predictions during HUT. The top two graphs depict the total blood volume during HUT without (left) and with (right) cardiovascular regulation. The following two graphs show cardiac output computed without (left) and with (right) cardiovascular regulation. Again, pulsatile (blue), pulsatile mean values (black), and non-pulsatile (red, dashed) denote simulations with nominal and (magenta) with estimated parameter values. The bottom graph shows estimated values for R_{aup} with pulsatile (magenta) and non- pulsatile (blue) models.

4 CONCLUSIONS

This study has shown that it is possible to develop a pulsatile and a non-pulsatile model that can both

predict dynamics during HUT, and that time-varying parameters (R_{aup}) can be predicted by both models. Moreover, we have shown (graph not included) that it is possible to use parameter estimates obtained with the non-pulsatile model within the pulsatile model. This could be used in simulations done over long time-scales (min-hours) where it may only be necessary to study pulsatility intermittently, e.g., following given events within the system. Finally, it should be noted that compartments and parameters associated with the arterial and venous subsystems are identical for the two models. The only difference is the compartment predicting dynamics of the left heart.

In summary, we have developed a non-pulsatile model and shown that it can be used to predict HUT dynamics. These models (the pulsatile and non-pulsatile models) have many potential benefits for the study of complex models, which contain a cardiovascular component. The advantage of results presented here is that the non-pulsatile model has potential to be included in for applications that require analysis of data over large time-scales.

ACKNOWLEDGEMENTS

Williams and Olufsen were supported in part by the virtual rat physiology project (VPR) supported by NIH-NIGMS under grant #1P50GM094503-01A0 sub-award to NCSU. Tran and Olufsen were also supported by NSF under the grant NSF/DMS #1022688.

REFERENCES

Batzel, J., Kappel, F., Schneditz, D., and Tran, H. (2007). *Cardiovascular and respiratory systems: modeling, analysis, and control*. SIAM, Philadelphia, PA.

Burton, A. (1972). *Physiology and biophysics of the circulation: an introductory text*. Year Book Medical Publishers Inc, Chicago, IL.

Ellwein, L. (2008). *Cardiovascular and respiratory modeling*. PhD thesis, Department of Mathematics, NC State University, Raleigh, NC.

Grodins, F. (1959). Integrative cardiovascular physiology: a mathematical synthesis of cardiac and blood vessel hemodynamics. *Q Rev Biol*, 34:93–116.

Hall, J. (2011). *Guyton and Hall Textbook of Medical Physiology*. Saunders, Philadelphia, PA, 12th edition.

Klabunde, R. (1972). *Physiology and biophysics of the circulation: an introductory text*. Lippincott Williams and Wilkins, Philadelphia, PA.

Lanier, J., Mote, M., and Clay, E. (2011). Evaluation and management of orthostatic hypotension. *Am Fam Physician*, 84:527–536.

Olufsen, M., Ottesen, J., Tran, H., Ellwein, L., Lipsitz, L., and Novak, V. (2005). Blood pressure and blood flow variation during postural change from sitting to standing: model development and validation. *J Appl Physiol*, 99:1523–1537.

Williams, N., Wind-Willassen, O., Program, R., Mehlsen, J., Ottesen, J., and Olufsen, M. (2013). Patient specific modeling of head-up tilt. *Math Med Biol*, In press.